Neutralization of Conservative Charged Transmembrane Residues in the Na^+/Glucose Cotransporter SGLT1†

Mariana Panayotova-Heiermann,* Donald D. F. Loo, Jason T. Lam, and Ernest M. Wright

Department of Physiology, University of California at Los Angeles Medical Center, Los Angeles, California 90095-1751

Received January 6, 1998; Revised Manuscript Received April 13, 1998

ABSTRACT: Our goal was to identify pairs of charged residues in the membrane domains of the Na^+/glucose cotransporter (SGLT1) that form salt bridges, to obtain information about packing of the transmembrane helices. The strategy was to neutralize Glu225, Asp273, Asp294, and Lys321 in helices 6−8, express the mutants in oocytes, measure [^{14}C]-αMDG uptake, and then attempt to find second-site mutations of opposite charge that restored function. αMDG uptake by E225A was identical to that by SGLT1, whereas transport was reduced by over 90% for D273A, D294A, and K321A and was not restored in the double mutants D273A/K321A or D294A/K321A. This suggested that K321 did not form salt bridges with D273 or D294 and that E225 was not involved in salt-bridging. Neutralization of K321 dramatically changed the Na^+ uniport and Na^+/glucose cotransport kinetics. The maximum rate of uniport in K321A increased 3−5-fold with a decrease in the apparent affinity for Na^+ ($\kappa_{0.5}^{Na^+}$ 70 vs 3 mM) and no change in apparent H^+ affinity ($\kappa_{0.5}^{H^+}$ 0.5 μM). The change in Na^+ affinity caused a +50 mV shift in the charge/voltage (*Q*/*V*) and relaxation time constant (τ)/voltage curves in the presteady-state kinetics. The presteady-state kinetics in H^+ remained unchanged. The lower Na^+ affinity resulted also in a 200-fold increase in the apparent $K_{0.5}$ for αMDG and phlorizin. Replacements of K321 with alanine, valine, glutamine, arginine, or glutamic acid residues changed the steady-state kinetics in a similar way. Therefore, we suggest that K321 determines, directly or indirectly, (i) the rate and selectivity of SGLT1 uniport activity and (ii) the apparent affinities of SGLT1 for Na^+, and indirectly sugar in the cotransport mode.

Understanding the relationship between structure and function of Na^+-dependent substrate transporters is of major importance, since this class of membrane proteins supplies cells with essential nutrients. Turk et al. (*1*, *2*) proposed that the secondary structure for the Na^+-dependent glucose cotransporter family (SGLT1)[1] is composed of 14 α-helical membrane spans. Charged and polar residues within the transmembrane domain could be involved in the SGLT conformational changes and/or Na^+ binding. However, since the presence of positive or negative charges in the dielectric environment of the membrane is energetically unfavorable, membrane charges often feature as partners in "charge-pair neutralization" with another membrane countercharge. Salt bridges have been reported for both globular α-helical proteins (*3*) and membrane proteins (*4*, *5*).

Here we have focused on charged residues in a highly conserved domain of SGLT1, i.e., in and around transmembrane helices 7 and 8. In this region (amino acids 273−336 in rabbit SGLT1) every positive (R300, K305, H309, K311, K321, K336) or negative (D273, D294) charge is conserved among all isoforms and homologous members of the family. The same region is a "hot spot" for mutations in human SGLT1 (W276L, C292Y, Q295R, R300S, and A304V; *6*−*8*) that cause glucose−galactose malabsorption. Even in *Vibrio parahaemolyticus* SGLT (*9*) residues K321, R300, and K305 are conserved. According to the SGLT1 topology model (*1*), amino acids E225, D273, and D294 reside adjacent to helix 8 and are potential candidates as charged-pair partners with K321 (Figure 1). Therefore we tested for interactions between K321 and E225, D273, or D294. Electrophysiological and flux analysis of rabbit SGLT1 and K321 mutants indicated that K321 modulates the Na^+ uniport and Na^+/sugar cotransport kinetics of SGLT1 but it does not form salt bridges with the residues D273, D294, or E225.

EXPERIMENTAL PROCEDURES

Molecular Biology. A construct containing the cDNA sequence for rabbit SGLT1 in pGEM3Zf+ (*10*) was used for subcloning of mutant PCR fragments. Mutations were directed by synthetic oligonucleotide primers applying a two-stage PCR protocol (*11*). The sequences of the mutagenic oligonucleotides are given in their 5′ → 3′ direction, and mutated nucleotides are presented in boldface letters and are underlined: E225A, CGTACCCTCCTACT**G**CTGGAAAAGCGAAAC; D273A, CCAAAGACGAGCC**C**GGGCCAGGGGATG**G**CCCCAGTGATGG; D294A, GCACAATGACCTGA**G**CAGTGCACCAGTACC; K321A, AGGAACAT-

† This research was supported by NIH Grants DK44602 and NS25554.

* Correspondence should be addressed to this author at Department of Physiology, UCLA Medical Center, CHS, Box 951751, Los Angeles, CA 90095-1751. Phone (310) 825-6905; FAX (310) 206-5661; E-mail mariana@physiology.medsch.ucla.edu.

[1] Abbreviations: SGLT1, high-affinity Na^+/glucose cotransporter; αMDG α-methyl D-glucopyranoside; Pz, phlorizin; $K_{0.5}$, concentration of αMDG, Na^+, or H^+ giving 50% of the maximum rate of cotransport; $\kappa_{0.5}$, concentration of Na^+ or H^+ giving 50% of the maximum rate of uniport.

S0006-2960(98)00039-7 CCC: $15.00
Published on Web 07/03/1998

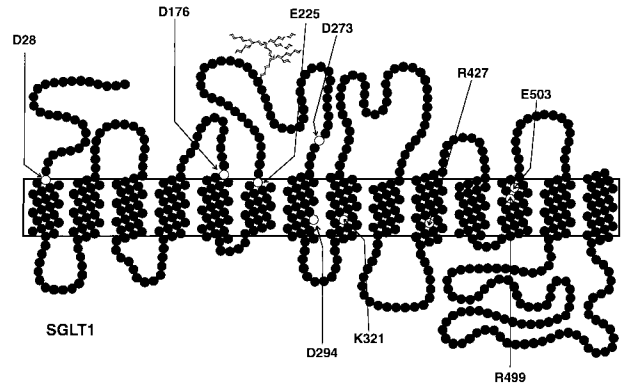

FIGURE 1: Secondary structure model for SGLT1 (*1*). Shown are the residues mutated in this study, E225, K321, D294, and D273, and those studied previously, D28, D176, R427, and R499 (*6*, *7*, *10*, *20*). Note that in an earlier secondary structure model D273 was predicted to be in the membrane.

AGGCATCACC**GC**CAGGTACCCACACAG; K321E, AGGAACATAGGCATCACCT**C**CAGGTACCCACACAG; K321R, AGGAACATAGGCATCACC**C**TCAGGTACCCACACAG; K321Q, AGGAACATAGGCATCACCT**G**CAGGTACCCACACAG; K321V, AGGAACATAGGCATCACC**AC**CAGGTACCCACACAG. To create the double mutant D273A/K321A, the recombinant D273A plasmid was cut with *Kpn*I/*Hinc*II and used as vector recipient. The plasmid construct for the K321A mutation was cut with the same restriction endonucleases and the DNA fragment was religated into the vector recipient. The double mutant D294A/K321A was obtained by introducing a *Stu*I/*Kpn*I fragment carrying the D294A mutation in the *Stu*I/*Kpn*I-cut plasmid with mutation K321A. All mutations and sequences of subcloned DNA were verified by sequencing with the Sequenase kit from U.S. Biochemical Corp. The mutagenic DNA templates were linearized with *Eco*RI and transcribed in vitro from the SP6 RNA polymerase promoter (MEGAscript kit, Ambion, Austin, TX).

Transport Assays and Electrophysiology. *Xenopus* oocytes were injected with 50 ng of either wild-type or mutant cRNA and kept at 18 °C for 5−10 days (*12*). Na^+-dependent αMDG uptake was measured by a radioactive tracer technique (*13*). Electrophysiological measurements were made with a two-microelectrode voltage clamp (*10*, *14*). To obtain current/voltage relationships, membrane voltage was stepped for 100−500 ms from the holding potential (V_h) to test potentials (V_t) ranging between −150 and +50 mV. Steady-state and presteady-state kinetic parameters were calculated by nonlinear regression analysis (see figure legends) by applying the fitting routines in ENZFITTER (Elsevier-Biosoft, Cambridge, U.K.) and Sigma Plot (Jandel Scientific, San Rafael, CA). All experiments were repeated at least three times with oocytes from different donor frogs.

RESULTS

Mutation of Charged Residues. We have neutralized E225, D273, D294, and K321 (Figure 1) by site-directed mutagenesis, expressed the mutants in oocytes, and measured [^{14}C]-αMDG uptake (Figure 2). Sugar transport was identical to that of the wild type for E225A, reduced more than 90% for D273A and K321A, and eliminated for D294A. The transport inhibition observed for D273A, K321A, and D294A was not restored in the double mutants D273A/K321A and D294A/K321A. Western blot analysis (not shown) verified that these mutant proteins were produced within the cell in amounts comparable to SGLT1. Electrophysiological analysis of both sugar-induced currents and presteady-state currents in the absence of sugar confirmed the uptake results and further demonstrated that (1) the kinetics of sugar transport for E225A was similar to those of the wild type ($K_{0.5}^{\alpha MDG} \sim 0.2$ mM, $K_i^{Pz} \sim 5$ μM), (2) the K321A protein was present in the plasma membrane (see below), and (3) there was little expression of D273A, D294A, or D273A/K321A in the oocyte plasma membrane, i.e., $Q_{max} < 2$ nC and $I_{max}^{\alpha MDG} < 100$ nA at 40−100 mM αMDG (*15*).

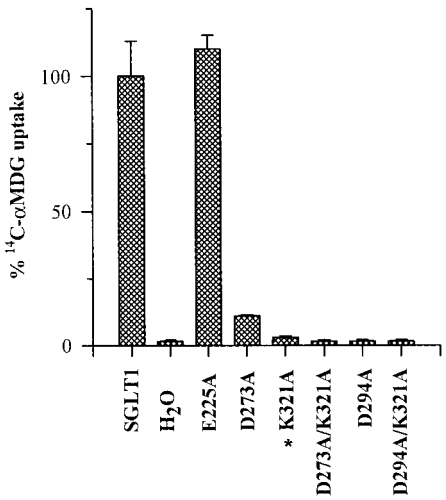

FIGURE 2: Total uptakes measured in 50 μM ^{14}C-αMDG. Sugar transport was assayed (*13*) in 50 μM of ^{14}C-αMDG, 4−7 days after injection of SGLT1 or mutant cRNA into the oocytes. The asterisk indicates sugar concentration of 100 μM. For each mutant the data were normalized to the sugar transport by SGLT1 in the same batch of oocyte. Errors represent SEM, $n = 4$.

K321A Steady-State Sugar Cotransport. Figure 3A shows the two components of the currents associated with SGLT1: a Na^+ "leak" in the absence of sugar and a sugar-induced steady-state inward Na^+ current. Shown are continuous currents from oocytes from the same donor expressing rbSGLT1 and K321A at −50 mV, when Na^+ and sugar were sequentially added to the external solution. The leak current was estimated by substitution of external Na^+ by choline and was greater for K321A (−130 nA) than for the wild-type (−55 nA). The current induced by 10 mM αMDG was much larger for wild type (−210 nA) than for K321A, even at 100 mM αMDG (−108 nA).

The current/voltage relations of the Na^+ leak and the sugar-induced current generated by SGLT1 and the mutant are shown in Figure 3. In both SGLT1 and K321A, the leak currents increased with voltage and $[Na^+]_o$ (5−100 mM). For SGLT1 this current saturated at the most negative potential (−150 mV), but for K321 the leak current showed a supralinear increase with hyperpolarization. For the two proteins, there was a difference in the ratio of the sugar-induced to the leak currents. For SGLT1 the current induced by 10 mM αMDG in 100 mM NaCl (−600 nA at −150 mV) was 1 order of magnitude larger than the current in the absence of sugar (−75 nA). In 15 oocytes expressing SGLT1 the Na^+ leak current was 18% ± 4% of the total current measured in the presence of saturating sugar. For K321A (Figure 3C) the leak current was comparable in

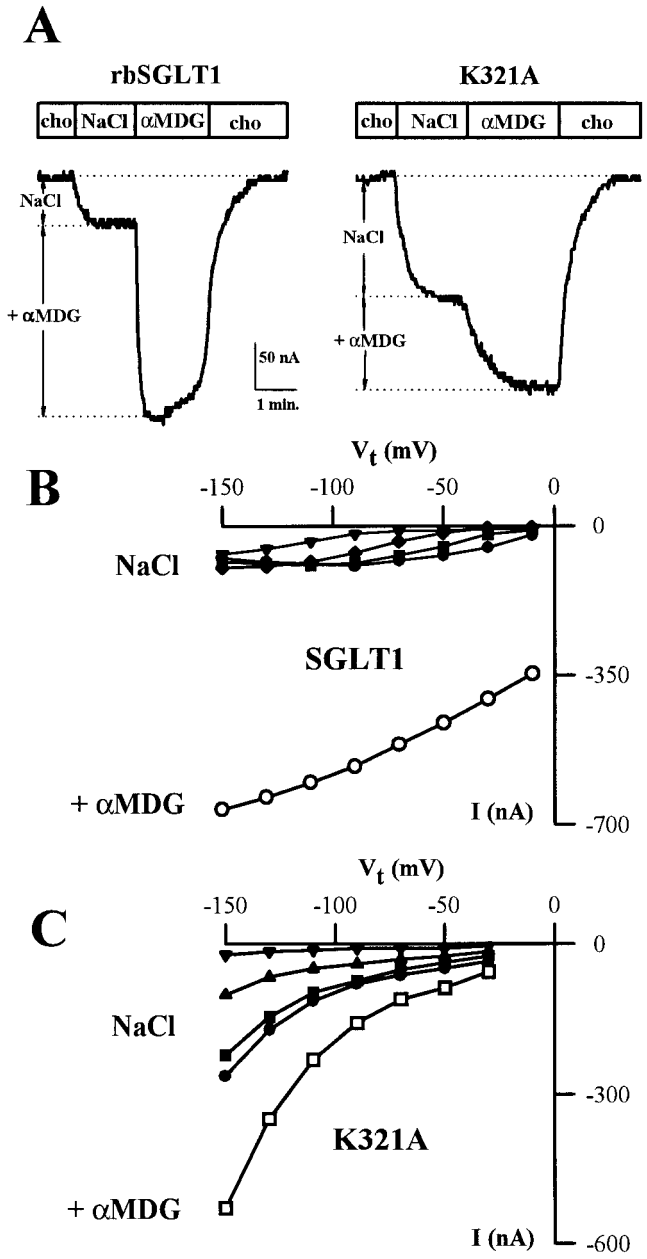

FIGURE 3: Current/voltage relationships for wild type and K321A. (A) Current records from single oocytes expressing rbSGLT1 and K321A showing αMDG-induced Na^+ inward currents. $V_h = -50$ mV. The dashed line represents the baseline in 100 mM choline chloride. Subsequent addition of 10 mM αMDG (rbSGLT1) or 100 mM αMDG (K321A) induced large inward currents. (B) Current/voltage (*I*/*V*) relationships of the rbSGLT1 steady-state currents. The curves for Na^+ uniport currents were obtained as the difference of the steady-state currents in the absence and presence of different $[Na^+]_o$: 5 (▼), 20 (◆), 50 (■), or 100 (●) mM. The *I*/*V* curve of the sugar-induced Na^+ inward currents (○) is the difference of the steady-state currents in the presence and absence of 10 mM αMDG. (C) *I*/*V* relationships of the K321A steady-state currents. *I*/*V* curves were obtained as described in panel B, except that $[Na^+]_o$ was 20 (▼), 60 (▲), 100 (■), and 150 (●) mM, and the αMDG-induced currents were measured in 100 mM αMDG (□).

magnitude to the sugar-induced current, 51% ± 4% (SEM, $n = 8$).

H^+ and Li^+ have been shown to be able to substitute for Na^+ in SGLT1, showing both Li^+ and H^+ leak and sugar-induced currents (*16*, *17*). For K321A addition of 100 mM αMDG to 100 mM LiCl or 3.16 μM H^+ (choline pH 5.5) generated only small currents (−110 nA at −150 mV).

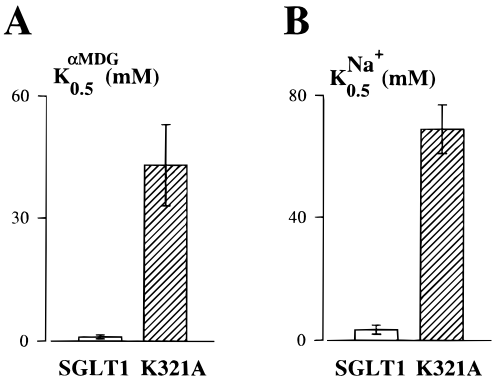

FIGURE 4: Na^+/sugar cotransport by wild-type and K321A. (A) Apparent affinities for αMDG in NaCl. The external Na^+ concentration $[Na^+]_o$ was fixed at 100 mM while the $[\alpha MDG]_o$ was varied. For wild type $[\alpha MDG]_o$ was (in millimolar) 0.015, 0.03, 0.06, 0.12, 0.25, 0.5, 1, 5, or 20; and for K321A (in millimolar), 0.5, 1, 5, 10, 20, 40, 60, 80, or 100. At each membrane potential the measured αMDG-induced currents were fitted to the equation $I = I_{max}^{\alpha MDG}[\alpha MDG]/(K_{0.5}^{\alpha MDG} + [\alpha MDG])$, where $I_{max}^{\alpha MDG}$ is the apparent maximal current at saturating αMDG concentrations and $K_{0.5}^{\alpha MDG}$ is the sugar concentration at 50% $I_{max}^{\alpha MDG}$. At −150 mV the $K_{0.5}^{\alpha MDG}$ was 0.2 ± 0.03 mM for wild type and 43 ± 10 mM for K321A. Error bars are standard errors of the fit; V_h was −50 mV. Similar parameters described two additional experiments. (B) Apparent affinities for Na^+. The αMDG-induced currents were measured as a function of $[Na^+]_o$. $[Na^+]_o$ was varied between 0 and 100 mM, whereas $[\alpha MDG]_o$ was maintained at 10 mM for SGLT1 and 100 mM for K321A. $[Na^+]_o$ for wild-type was (in millimolar) 0, 5, 10, 20, 50, 70, or 100 and for K321A (in millimolar) 0, 2.5, 5, 10, 20, 40, 60, 70, 80, 90, or 100. The sugar-dependent Na^+ currents were fitted to the Hill equation $I = I_{max}^{Na^+}[Na^+]_o^n/((K_{0.5}^{Na^+})^n + [Na^+]_o^n)$. $I_{max}^{Na^+}$ is the maximal current at saturating Na^+ concentrations, $K_{0.5}^{Na^+}$ is the value of $[Na^+]_o$ at 50% $I_{max}^{Na^+}$, and n is the Hill coefficient for Na^+. $K_{0.5}^{Na^+}$ at −150 mV was 69 ± 8 mM for K321A and 3.5 ± 1.5 mM for SGLT1.

Given the magnitude of the leak currents, up to −1600 nA, it was not possible to obtain cotransport kinetics for K321A in Li^+ or H^+.

Figure 4 summarizes the apparent affinity constants $K_{0.5}$ for sugar and Na^+. $K_{0.5}^{\alpha MDG}$ for K321A (43 ± 10 mM at −150 mV) was approximately 200-fold higher than for SGLT1. At −150 mV the $K_{0.5}^{Na^+}$ for SGLT1 was significantly lower (3.5 ± 1.5 mM in 10 mM αMDG) than that for K321A (69 ± 8 mM in 100 mM αMDG). The Hill coefficients were 1.4 ± 0.5 for K321A and 1.8 ± 0.5 for SGLT1 (errors represent errors of the fit). The $K_{0.5}^{Na^+}$ for wild-type and mutant proteins were slightly voltage-dependent, increasing to 10 ± 5 mM and 76 ± 14 mM at −50 mV. In this pair of experiments, $I_{max}^{Na^+}$ was −290 ± 20 nA for K321A and −590 ± 50 nA for SGLT1. In a second series for K321A the $K_{0.5}^{Na^+}$ was 53 ± 5 mM and the Hill coefficient was 1.9 ± 0.2

Leak Pathway. Figure 5 shows the apparent affinity constants for Na^+ and H^+ leaks through SGLT1 and K321A. The $\kappa_{0.5}$ values for Na^+ ($\kappa_{0.5}^{Na^+}$) or H^+ ($\kappa_{0.5}^{H^+}$) were obtained by fitting the steady-state inward currents to the Hill equation (Figure 4B). The $\kappa_{0.5}^{Na^+}$ for SGLT1 was 2.5 ± 0.9 mM at −150 mV, whereas $\kappa_{0.5}^{Na^+}$ for K321A at this voltage was 71 ± 5 mM. The Na^+ Hill coefficient for K321A was 3.1 ± 0.6 (2.1 ± 0.2 for rbSGLT1) and $I_{max}^{Na^+}$ was −290 ± 23 nA (−98 ± 2 nA for rbSGLT1).

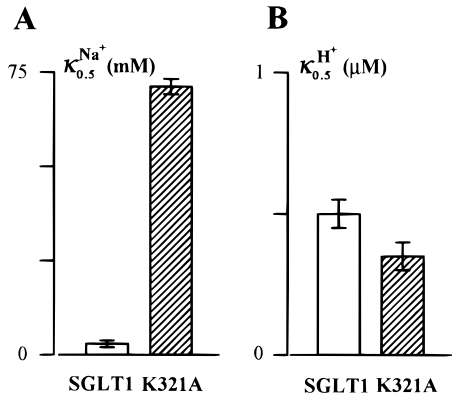

FIGURE 5: Leak pathway for SGLT1 and K321A. (A) Apparent affinities for the sugar-independent Na^+ currents ($\kappa_{0.5}^{Na^+}$). In the absence of αMDG, the $[Na^+]_o$ for wild-type and K321A was varied between 0 and 100 mM $[Na^+]_o$ and the difference of the currents in Na^+ and choline was fitted to the Hill equation (Figure 3B). At −150 mV $\kappa_{0.5}^{Na^+}$ for SGLT1 was 2.5 ± 0.9 mM, and for K321A, 71 ± 5 mM, SEM, $n = 3$. (B) Apparent affinities for the sugar-independent H^+ current ($\kappa_{0.5}^{H^+}$). External $[H^+]_o$ were 0.031, 0.1, 0.316, 1.0, and 3.16 μM. $\kappa_{0.5}^{H^+}$ for SGLT1 was 0.51 ± 0.04 μM ($n = 2$), and for K321A it was 0.35 ± 0.04 μM ($n = 5$).

Increasing the external H^+ concentration from 0.0316 to 10 μM induced K321A leak currents up to −1800 nA, with an apparent $\kappa_{0.5}^{H^+} = 0.35 \pm 0.04$ μM and Hill coefficient of 1.8 ± 0.1, at −150 mV (SEM, $n = 5$). Calculated $I_{max}^{H^+}$ values at −150 mV for K321A were between −400 and −1800 nA, and for rbSGLT1, −200 to −300 nA. The results obtained on oocytes expressing rbSGLT1 were similar, i.e., $\kappa_{0.5}^{H^+} = 0.51 \pm 0.04$ μM, $I_{max}^{H^+} = -253 \pm 16$ nA, and $n = 1.4 \pm 0.32$ (Figure 4B). Inward leak currents were also detected in 100 mM LiCl (−100 to −600 nA at −150 mV) for SGLT1 and K321A, and the magnitude of the leak currents were in the sequence $H^+_{leak} > Li^+_{leak} > Na^+_{leak}$ for both the wild-type and mutant proteins.

Are the changes in kinetics observed for K321A caused by the inserted alanine or by the loss of the lysine at this position? To answer this question we replaced K321 with charged (K321R, K321E), polar (K321Q), or neutral (K321V) residues. The conservative substitution K321R caused a phenotype close to that of K321A. The Na^+ currents had the same amplitude as the αMDG-induced inward currents: −138 nA in the presence and −126 nA in the absence of 100 mM αMDG at −150 mV, with an increase of $\kappa_{0.5}^{Na^+}$ to 51 ± 10 mM and $K_{0.5}^{\alpha MDG}$ to 64 ± 29 mM at −150 mV. The errors of the fits illustrated that 100 mM NaCl and 150 mM sugar were not sufficient to saturate transport. Similarly to K321A, the K321R mutant steady-state kinetics in protons were close to these for SGLT1 ($\kappa_{0.5}^{H^+} = 0.74 \pm 0.06$ μM, $I_{max}^{H^+} = -679 \pm 34$ nA, $n = 1.5 \pm 0.15$, and $V_t = -150$ mV). Addition of 100 mM αMDG inhibited the inward H^+ leak currents by 30−50 nA. Similar results were observed for K321E, K321Q, and K321V mutants ($\kappa_{0.5}^{Na^+} > 80$ mM Na^+, $K_{0.5}^{\alpha MDG} > 100$ mM αMDG). For these mutants the H^+ affinity remained in the range typical for SGLT1. $\kappa_{0.5}^{H^+}$ varied between 0.72 ± 0.1 μM (K321E) and 1.3 ± 0.1 μM (K321V) with $I_{max}^{H^+} > -1000$ nA and $n > 1$ at $V_t = -150$ mV.

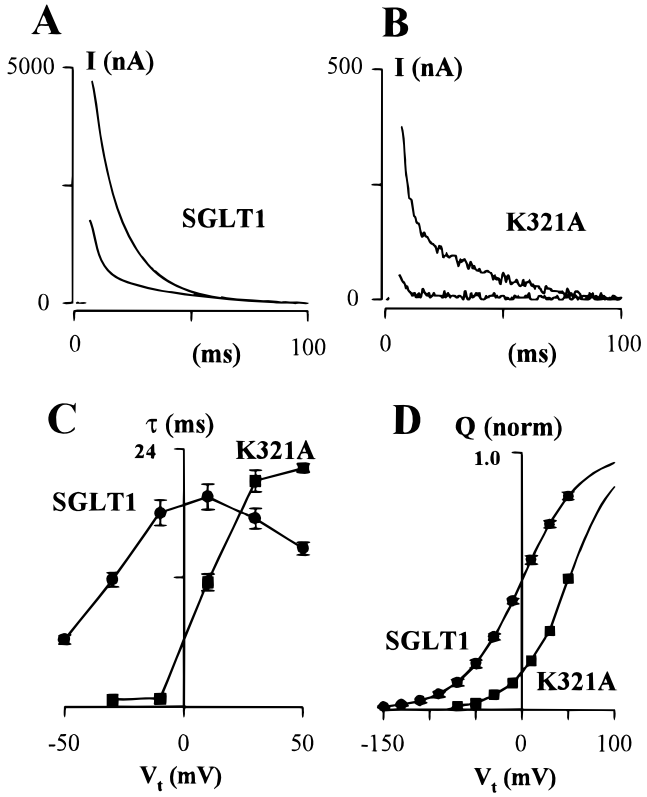

FIGURE 6: Presteady-state charge translocations associated with rbSGLT1 and K321A. (A) Presteady-state currents from a SGLT1-expressing oocyte where the membrane voltage was held at −100 mV and then jumped for 100 ms to +50 (upper trace) and −10 mV (lower trace). (B) Same recording as presented in panel A but from an oocyte expressing K321A. (C) Kinetics of the presteady-state current relaxation. The time constants of relaxation in 100 mM NaCl for the on-current transients (τ) for each tested membrane potential (V_t) were obtained by fitting the measured current (I) to the equation $I = I_1 e^{-t/\tau_1} + I e^{-t/\tau} + I_{ss}$, where I_1 is the oocyte capacitive current with time constant τ_1, I is the K321A transient current with time constant τ, before decaying to the steady-state current (I_{ss}). (D) Charge/voltage relationship of the current transients. The integrals of the off-transient currents (Q) due to K321A were plotted as a function of the applied test voltage V_t. The smooth curve was obtained by fitting the charge/voltage relationship at $[Na^+]_o = 100$ mM to the Boltzmann equation: $(Q - Q_{hyp}) = Q_{max}/[1 + \exp(V_t - V_{0.5})zF/RT]$. $Q_{max} = (Q_{dep} - Q_{hyp})$ is the maximal charge transfer, Q_{dep} and Q_{hyp} are the charge movements at the depolarizing and hyperpolarizing limits, $V_{0.5}$ is the potential for 50% Q_{max}, z is the apparent valence of the movable charge, and F, R, and T have their usual meanings.

Presteady-State Currents. In the absence of sugar, K321A and SGLT1 exhibited presteady-state currents after step changes in membrane voltage in both Na^+ (Figure 6A,B) and H^+ (not shown). For K321A the relaxation of the current transients in Na^+ was described by a monoexponential function with a time constant (τ) of 22 ms at +50 mV. In 100 mM Na^+ τ followed a bell-shaped relationship to V_m (Figure 6C), similar in shape to SGLT1, but with a peak at a more positive V_m [$\tau_{max} \sim$ +50 mV vs ∼1 mV (*10*)]. Lowering the external $[Na^+]_o$ to 10 mM shifted the voltage for τ_{max} from K321A to −37 mV, comparable to the shift for SGLT1 (*18*).

The charge/voltage (Q/V) relationship in 100 mM $[Na^+]_o$ did not saturate at positive potentials for K321A (Figure 6D) and so evaluation of the Boltzmann parameters (Q_{max}, maximal charge transferred; z, apparent valence of the charge transferred; and $V_{0.5}$,voltage for 50% Q_{max}) was performed

Table 1: Summary of Parameters Describing Steady-State Kinetics at $V_t = -150$ mV

affinities	conditions	rabbit SGLT1	K321A
$\kappa_{0.5}^{Na^+}$	−αMDG	2.5 ± 0.9 mM	71 ± 5 mM
$K_{0.5}^{Na^+}$	+αMDG	3.5 ± 1.5 mM (10 mM αMDG)	69 ± 8 mM (100 mM αMDG)
$\kappa_{0.5}^{H^+}$	−αMDG	0.51 ± 0.04 μM	0.35 ± 0.04 μM
$K_{0.5}^{\alpha MDG}$	Na^+	0.2 mM	43 mM
κ_i^{Pz}	Na^+ −αMDG	1.5 ± 0.5 μM	850 ± 50 μM
K_i^{Pz}	Na^+ +αMDG	1 μM (100 mM αMDG)	700 μM (100 mM αMDG)
κ_i^{Pz}	H^+ −αMDG	10 μM	≈80 μM

at lower Na^+ concentrations. At lower Na^+ the Q/V curve shifts into a working range (see ref *18*). The kinetic parameters of charge transfer at 10 mM NaCl in an oocyte with $I_{max}^{\alpha MDG} = -170$ nA at −150 mV were $V_{0.5} = -37 \pm 3$ mV, $Q_{max} = 13 \pm 0.8$ nC, and $z \sim 1$. The SGLT1 values at 10 mM Na^+ were $V_{0.5} = -88$ mV, $Q_{max} = 13$ nC, and $z = 1.1 \pm 0.1$ ($n = 4$) (*18*).

The apparent cotransporter turnover rates for SGLT1 isoforms, defined by the ratio $I_{max}^{\alpha MDG}$ at −150 mV to Q_{max} at saturating Na^+ vary in the range from 25 s^{-1} for rabbit SGLT1 (30 s^{-1} for rat SGLT1) to 57 s^{-1} for human SGLT1 (*14*). The cotransporter turnover rate for K321A was ≥15 s^{-1} (at 10 mM NaCl, $I_{max}^{\alpha MDG}/Q_{max} = -170$ nA/13 nC; at 20 mM NaCl, $I_{max}^{\alpha MDG}/Q_{max} = -236$ nA/16 nC).

At pH 5.5 in choline chloride the presteady-state currents for SGLT1 and K321A relaxed with comparable time constants (∼170 ms at −150 mV). For both proteins the transient currents relaxed faster with more positive voltages and reached 35 ms (K321A) and 40 ms (rbSGLT1) at +50 mV. τ_{off} was independent of voltage between −150 mV and +50 mV (100 ms for K321A; 60 ms for rbSGLT1). The charge moved by the SGLT1 at pH 5.5 during the onset of the pulse was described by a Boltzmann relation with $V_{0.5} = -52$ mV, $z = 1.0 \pm 0.1$, and $Q_{max} = 10$ nC. Therefore the cotransport turnover number for SGLT1 in H^+ ($I_{max}^{\alpha MDG}/Q_{max}$) was >35 s^{-1}. The presteady-state parameters measured on an individual K321A expressing oocyte as determined from the OFF transients were $V_{0.5} = -58$ mV, $z = 0.6 \pm 0.05$ and $Q_{max} = 37$ nC.

Phlorizin. The plant glucoside phlorizin is a competitive blocker of Na^+/glucose cotransport, charge translocation, and the leak pathway. Its apparent inhibitory constant (K_i^{Pz}) estimated in the presence of saturating sugar (5 mM αMDG) for rbSGLT1 in Na^+ is ∼1 μM (*12*) and in protons ∼10 μM (*19*); see Table 1. The apparent κ_i for phlorizin inhibition of the leak pathway in 3.16 μM protons was 8.5 ± 0.5 μM ($n = 2$) for SGLT1 and 88 ± 11 μM ($n = 3$) for K321A. The apparent $\kappa_{0.5}^{Pz}$ for the SGLT1 Na^+ leak current was 1.5 ± 0.5 μM ($n = 2$) and 850 ± 50 μM ($n = 3$) for K321A. The apparent K_i^{Pz} values for Na^+/αMDG cotransport were ∼700 μM for K321A and ∼1 μM for the wild type (Table 1).

DISCUSSION

The structural determinant(s) of the Na^+/glucose cotransporter function has become an intense area of investigation, with approaches ranging from site-directed mutagenesis (*10*, *20*) and construction of chimeras (*21*) to truncation of the protein (*22*) and the study of functional defects in mutant proteins found in patients with glucose−galactose malabsorption (*7*, *8*). These studies suggest that the C-terminal five helices of the protein determine sugar selectivity, affinity, and permeation (*21*, *22*).

Another powerful approach to study the helical packing of membrane proteins is to identify pairs of charged residues in hydrophobic domains (*4*, *5*). The strategy is to identify functionally important charged residues, neutralize them by site-directed mutagenesis, and find second-site mutations of oppositely charged residues that restore function. In this study we have neutralized two charged residues (K321A and D294A) in transmembrane helices 7 and 8, a highly conserved region in the SGLT1 gene family (*2*), and examined the function of the mutant proteins. The D294A mutant was not functionally expressed in the plasma membrane and function was not restored in the double mutant D294A/K321A. This suggests that D294 does not form a salt bridge with K321 and rescue trafficking to the plasma membrane and functional activity. Mutation of E225 at the extracellular end of helix 6 did not affect the kinetics of SGLT1, suggesting that this residue is not involved in intramolecular salt bridging. As anticipated, there is no interaction between K321 and another acidic residue, D273, in the hydrophilic loop between helices 6 and 7. While neutralization of D273 reduced transport activity below 10% of wild type due to a trafficking defect, there was no significant transport by the double mutant D273A/K321A; i.e., the trafficking defect in D273 is not due to disruption of a salt bridge with K321.

According to the secondary structure model (Figure 1), there is only one other acidic residue in the hydrophobic interior of SGLT1: E503 in helix 12. However, this residue is more likely to form an intramembrane charged pair with R499 than with K321. Neutralization of R499 reduced both the delivery of the cotransporter to the plasma membrane and its affinity for sugar (*7*). Previous studies (*20*) also demonstrated that neutralization of R427 in helix 10 eliminated transport due to a trafficking defect. Although it cannot be excluded that mutant R427A is incorrectly folded due to disruption of a potential salt bridge, preliminary results suggest that the negatively charged counterpart of R427 is probably not residue D273. The double mutant D273A/R427A remained silent after addition of 5−10 mM αMDG. It is also highly unlikely that K321 is potentially involved in electrostatic interactions with the negatively charged D176 in helix 5, since a negative charge at this position is not necessarily required for cotransporter function (*10*). The first described case of glucose−galactose malabsorption on molecular level was the mutation of aspartate 28 (D28) in human SGLT1 (*6*). Replacement of D28 with other amino acids (D28N, D28Q, D28E, and D28A) reduced dramatically the sugar transport (K. Hager and E. M. Wright, unpublished observations). This suggests that the residue at position 28 is not involved in salt bridging.

The kinetics of Na^+/glucose cotransport were dramatically changed by the K321A mutation: the apparent affinity for sugar decreased by 200-fold ($K_{0.5}^{\alpha MDG}$ increased from 0.2 to 43 mM) and the apparent affinity for Na^+ decreased by a

comparable amount ($K_{0.5}^{Na^+}$ increased from 3.5 to 69 mM) (Table 1). The apparent inhibitory constant for phlorizin (Table 1) also increased from 1 to 700 μM. The increase in $K_{0.5}^{Na^+}$ for the mutant was identical to that for Na^+ uniport (see below), and we suggest that the decrease in Na^+ affinity accounts for the decrease in sugar and phlorizin affinity. This indicates that K321 is, directly or indirectly, involved in determining the Na^+ affinity of both the uniport and cotransport functions of SGLT1 and the magnitude of the Na^+ leak. The $I_{max}^{\alpha MDG}/Q_{max}$ ratios indicate that the K321A mutation does not alter the cotransport turnover number (>25 s^{-1}). Although Li^+ and H^+ are both able to drive sugar cotransport through SGLT1 (*16*, *17*) and K321A, it was not possible to carry out kinetic analysis of Li^+ and H^+ cotransport by the mutant simply because the currents induced by 100 mM αMDG were too small relative to the uniporter currents.

The SGLT1 leak pathway was first identified as a phlorizin-sensitive, Na^+-dependent current in the absence of sugar (*23*), and it is now recognized that leak currents are a common feature of cotransporters (*24*). More recently it has been demonstrated that the SGLT1 leak current is carried by Na^+ (*25*) and that H^+ can substitute for Na^+ in both leak and cotransport (*16*). The present study further demonstrates that the leak (i) is saturable ($\kappa_{0.5}^{Na^+}$ = 2.5 mM, $\kappa_{0.5}^{H^+}$ = 0.5 μM), (ii) exhibits Hill coefficients >1 for both Na^+ and H^+, and (iii) has a cation selectivity in the order H > Na > Li at −150 mV. The turnover number for the Na^+ leak was about 5 s^{-1} ($I_{max}^{Na^+}$ at −150 mV/Q_{max}), about 20% of that for Na^+/glucose cotransport (25 s^{-1}), consistent with the six-state model for SGLT1 (*26*). The turnover number for the H^+ leak was higher than for Na^+, but how much higher is unknown because the H^+ *I*/*V* curve did not saturate at −150 mV. Additional evidence suggesting that the leak is a uniporter is that the activation energy for the leak is 30 kcal/mol (*27*).

The leak currents for K321A were 3−5 times higher than for SGLT1 in both Na^+ and H^+ (Figure 3A). However, the $\kappa_{0.5}^{Na^+}$ increased from 3 to 70 mM while $\kappa_{0.5}^{H^+}$ did not change (0.4 vs 0.5 μM) (Table 1). This suggests that K321 modulates, directly or indirectly, the Na^+/H^+ selectivity and turnover of the uniport activity. The Na^+ turnover number was higher for K321A than for SGLT1 (>20 vs 5 s^{-1}). Analysis of the presteady-state currents for K321A showed that in 100 mM Na^+ the $V_{0.5}$ and the voltage for τ_{max} move +50 mV compared to SGLT1, whereas there was no difference in τ_{max} between the presteady-state currents for K321A and wild-type (Figure 6). Parenthetically, the 1000-fold higher affinity for the H^+ uniport than for Na^+ uniport (1 μM vs 3 mM) and the 10-fold difference in τ (100−200 ms vs 1−20 ms) may be explained by an increase in the rate constant for H^+ binding (k_{12}) and a decrease in the rate constant for H^+ dissociation (k_{21}). Phlorizin, the specific Na^+-dependent inhibitor of Na^+/glucose cotransport (*14*, *19*), is also a potent blocker of SGLT1 uniport activity (*23*). The κ_i^{Pz} values were 1.5 and 10 μM for the Na^+ and H^+ currents through SGLT1 and 850 and 80 μM for K321A (Table 1). The decrease in phlorizin affinity for K321A in the presence of Na^+ is consistent with the decrease in Na^+ affinity, while the decrease in the H^+ affinity might suggest a direct effect on phlorizin binding.

On the basis of the decrease of the apparent affinity for Na^+ by K321A, one would expect that there would be a shift of the τ/V and Q/V relations toward more negative potentials. However, it is important to keep in mind that there are two alterations that could affect K321A presteady-state currents: (1) the decrease in the Na^+ binding and (2) the large increase in the Na^+ leak. Computer simulations of our six-state kinetic model for Na^+/glucose cotransport (*26*) showed that while a decrease in Na^+ binding at the external membrane surface shifts the τ/V and Q/V curves to negative potentials, the greater effect is caused by the decrease in Na^+ binding at the internal membrane surface. Such a decrease predicts a shift of the τ/V and Q/V relations to positive potentials as observed in Figure 6C,D and would also account for the supralinearity of the Na^+ leak and steady-state *I*/*V* curves of the sugar-coupled current (Figure 3C).

In summary, this study of charged residues in the most highly conserved region of SGLT1 does not provide evidence for salt bridges between K321 and E225, D273, or D294. However, replacement of K321 with alanine, valine, glutamic acid, glutamine, or arginine showed that this lysine residue, directly or indirectly, plays a major role in both determining the turnover and cation selectivity of SGLT1 uniport activity and the Na^+ and sugar binding during cotransporter activity. The kinetics of the currents recorded in the absence of substrate provide evidence that the leak currents are due to SGLT1 behaving as a uniporter with 2 cations transported/cycle. This is consistent with the predictions of the six-state model (*26*).

ACKNOWLEDGMENT

We thank Dr. I. Foster for his insights into the interpretation of mutant presteady state kinetics and Ms. Manuela Contreras for her assistance with the oocytes.

REFERENCES

1. Turk, E., Kerner, C. J, Lostao, M. P., and Wright, E. M. (1996) *J. Biol. Chem. 271*, 1925−1934.
2. Turk, E., and Wright, E. M. (1997) *J. Membr. Biol. 159*, 1−20.
3. Rashin, A., and Honig, B. (1984) *J. Mol. Biol. 173*, 515−521.
4. Shahin-Tóth, M., Dunten, R. L., Gonzalez, A., and Kaback, H. R. (1992) *Proc. Natl. Acad. Sci. U.S.A. 89*, 10547−10551.
5. Dunten, R. L., Sahin-Toth, M., and Kaback, H. R. (1993) *Biochemistry 32*, 3119−3145.
6. Turk, E., Zabel, B., Mundlos, S., Dyer, J., and Wright, E. M. (1991) *Nature (London) 350*, 354−356.
7. Martín M., Turk, E., Lostao, M. P., Kerner, C., and Wright, E. M. (1996) *Nat. Genet. 12*, 216−220.
8. Martin, M. G., Lostao, M. P., Turk, E., Lam, J., Kreman, M., and Wright, E. M. (1997) *Gastroenterology 112*, 206−1212.
9. Sarker, R. I., Okabe, Y., Tsuda, M., and Tsuchiya, T. (1996) *Biochim. Biophys. Acta 1281*, 1−4.
10. Panayotova-Heiermann, M., Loo, D. D. F., Lostao, M. P., and Wright, E. M. (1994) *J. Biol. Chem. 269*, 21016−21020.
11. Landt, O., Grunert, H.-P., and Hahn, U. (1990) *Gene 96*, 125−128.
12. Parent, L., Supplisson, S., Loo, D. D. F., and Wright, E. M. (1992) *J. Membr. Biol. 125*, 49−62.
13. Ikeda, T. S., Hwang, E.-S., Coady, M. J., Hirayama, B. A., Hediger, M. A., and Wright, E. M. (1989) *J. Membr. Biol. 110*, 87−95.

14. Panayotova-Heiermann, M., Loo, D. D. F., and Wright, E. M. (1995) *J. Biol. Chem. 270*, 27099−27105.
15. Zampighi, G. A., Kreman, M., Boorer, K. J., Loo, D. D. F., Bezanilla, F., Chandy, G., Hall, J. E., and Wright, E. M. (1995) *J. Membr. Biol. 148*, 65−78.
16. Hirayama, B. A., Loo, D. D. F., and Wright, E. M. (1994) *J. Biol. Chem. 269*, 21407−21410.
17. Hirayama, B. A., Loo, D. D. F., and Wright, E. M. (1997) *J. Biol. Chem. 272*, 2110−2115.
18. Hazama, A., Loo, D. D. F., and Wright, E. M. (1997) *J. Membr. Biol. 155*, 175−186.
19. Hirayama, B. A., Lostao, M. P., Panayotova-Heiermann, M., Loo, D. D. F., Turk, E., and Wright, E. M. (1996) *Am. J. Physiol. 270*, G919−G926.
20. Lostao, M. P., Hirayama, B. A., Panayotova-Heiermann, M., Sampogna, S. L., Bok, D., and Wright, E. M. (1995) *FEBS Lett. 377*, 181−184.
21. Panayotova-Heiermann, M., Loo, D. D. F., Kong, C.-T., Lever, J. E., and Wright, E. M. (1996) *J. Biol. Chem. 271*, 10029−10034.
22. Panayotova-Heiermann, M., Eskandari, S., Turk, E., Zampighi, G. A., and Wright, E. M. (1997) *J. Biol. Chem. 272*, 20324−20327.
23. Umbach, J. A., Coady, M. J., and Wright, E. M. (1990) *Biophys. J. 57*, 1217−1224.
24. Wright E. M., Loo, D. D. F., Turk, E., and Hirayama, B. A. (1996) *Curr. Opin. Cell Biol. 8*, 468−473.
25. Mackenzie, B., Loo, D. D. F., and Wright, E. M. (1998) *J. Membr. Biol. 162*, 101−106.
26. Parent, L., Supplisson, S., Loo, D. D. F., and Wright, E. M. (1992) *J. Membr. Biol. 125*, 63−79.
27. Loo, D. D. F., Hirayama, B. A., Zeuten, T., Meinild, A.-K., and Wright, E. M. (1998) *FASEB J. 12*, A1017.

BI9800395